Chemical Engineering Journal 170 (2011) 194–201

Contents lists available at ScienceDirect

Chemical Engineering Journal

journal homepage: www.elsevier.com/locate/cej

Preparation and characterization of low energy post-pyrolysis oxygenated tire char

Augustine Quek, Rajasekhar Balasubramanian*

Division of Environmental Science & Engineering, Faculty of Engineering, National University of Singapore, Block E1A #02-19, 1 Engineering Drive 2, Singapore 117576, Singapore

ARTICLE INFO

Article history:
Received 11 January 2011
Received in revised form 8 March 2011
Accepted 10 March 2011

Keywords:
Pyrolysis
Tire
Oxygenation
Sorption
Copper

ABSTRACT

Char surfaces, obtained from pyrolysis of waste tires, were chemically modified *in situ* using a novel process of post-pyrolysis oxygenation. To enhance the adsorptive characteristics of pyrolytic char, low concentrations of oxygen were introduced into the pyrolysis reactor at various temperatures immediately after the pyrolysis process, without additional energy input. The chemically modified char was characterized using a range of analytical instruments. Proximate analysis showed a high amount of ash material in the chars after pyrolysis. X-ray photoelectron spectroscopy (XPS) and bulk metal content analysis showed that a high proportion of the char contained zinc. Pyrolysis of tires enriched the surface of the resultant chars with zinc through depolymerization and volatization of carbon and other organic compounds. Subsequent oxygenation of the chars resulted in the formation of zinc oxide (ZnO) and oxygenated carbon functional groups. Surface areas and pore sizes of the chars were relatively low. These characteristics were then correlated with aqueous copper removal through batch equilibrium studies. Surface atom abundance was found to be highly correlated with copper removal, but not surface areas. This characterization study further revealed that tire char surfaces tend to behave like graphite surfaces in their interaction with oxygen molecules during activation, while the presence of zinc on the char surface played an important role in copper removal.

1. Introduction

Activated carbon (AC) has been recognized by the scientific community as a non-graphitic, amorphous, carbon-based material with a large internal surface area and pore volumes. Theoretically, active carbons can be prepared from any carbonaceous materials [1]. However, only a few sources of low-cost raw materials such as coal, lignite, wood, coconut shell and some agricultural waste are currently used for AC preparation due to high manufacturing costs. According to recent estimates, the world demand for AC is set to rise by 5.2% annually through 2012 to 1.15 million tonnes [2]. Thus, new sources of AC are continuously being explored.

Waste tires represent a potential source of AC, with an estimated 1.3 billion waste tires produced annually worldwide [3]. Pyrolysis has been shown to be a technically feasible method for producing AC from waste tires [4–26]. The rubber polymers break down and volatize under an inert atmosphere and high temperatures, leaving behind an active char that can be further processed into AC. Various reactor designs and technologies have been proposed [27–32] to produce a range of products such as oils, gases and solid char from the pyrolysis of tires. These include fixed beds [27,28], fluidized beds [29,30], spouted beds [31] and rotary kiln [32], operating under various conditions of temperature, heating rates, residence times and carrier gas. However, neither heating rates [15] nor pyrolysis temperatures above 500 °C generally seem to affect the yield of the char [11].

Tire chars can be activated by either a physical or chemical process. Physical activation exposes the carbonized char to oxidizing atmospheres (carbon dioxide, oxygen, or steam) at temperatures usually in the range of 600–1200 °C [1,8,11,12,15–19,23,24]. Chemical activation uses activating agents such as sodium sulfide [10], potassium hydroxide [14], sodium hydroxide [25], sulfuric acid [9,20,21,25], phosphoric acid [14], and zinc chloride [14,20,21]. These activations were done mainly to modify surface properties of the carbons such as the carbon structure, pore sizes and surface areas.

Oxidation processes have received considerable attention in recent years for AC preparation and activation [1,12,18,26,33]. Suuberg and Aarna [12] activated pyrolyzed tire char with various concentrations of oxygen gas and at different temperatures. They reported that the porosity of the tire chars was independent of the activation temperature and oxygen partial pressure. They also found that oxygen is least effective among the oxidative gases in developing porosity [12]. However, Helleur et al. [18] reported that Cu(II) adsorption capacity of pyrolytic char was thrice as much as that for commercial AC when the char was carbonized at 600 °C,

* Corresponding author. Tel.: +65 65165135; fax: +65 67744202.
E-mail address: eserbala@nus.edu.sg (R. Balasubramanian).

1385-8947/$ – see front matter © 2011 Elsevier B.V. All rights reserved.
doi:10.1016/j.cej.2011.03.053

even though the latter had more than twice the surface area of the former. There was also an improvement in lead adsorption when 2% oxygen was used during activation [18]. The enhanced sorption characteristics of the pyrolytic carbon were due to the chemisorption of oxygen, which is known to occur rapidly at high temperatures between 300 and 420 °C [34]. The evaluation of the chemisorbed oxygen on char surfaces can be done through a range of spectroscopic techniques [6,7,34].

In this work, chars were prepared by pyrolyzing waste rubber tires at 550 °C. The chars were then activated using low concentration oxygen by bleeding air into the reactor with no additional energy input. Different degrees of oxygenation on the char surfaces could be achieved at different temperatures of oxygenation. No additional energy was used in this post-pyrolysis oxygenation (PPO) process. Surface characterization was done on unactivated chars and pyrolyzed tire chars activated in the low-oxygen atmosphere. Proximate analysis, metal content analysis, XPS, SEM, and Brunauer–Emmett–Teller (BET) surface area determination were carried out to study the chemical and morphological characteristics of unactivated and activated pyrolyzed chars. Results indicated that the pyrolysis of tires together with *in situ* activation process with oxygen could enrich the char surface with oxygenated groups. The formation of zinc oxide (ZnO) on the char surface also appeared to change its surface chemistry. The active surface chemistry of the char was also demonstrated through the variation in aqueous copper removal from water with the variation in Zn and O surface groups on the chars.

2. Experimental

2.1. Material

The carbon char used in this study was obtained from the pyrolysis of scrap car tires which, in turn, were acquired from a local tire reuse plant. The scrap tires were shredded and steel wires were removed at the plant. The shredded tires were further cut into small particles of around 1 mm size before using them for pyrolysis.

2.2. Pyrolysis and activation

The pyrolysis of scrap tire samples was done in a horizontal tubular reactor with a N_2 gas flow rate of 0.6–0.8 L per min, at a heating rate of 20 °C per min, until 550 °C was reached. The temperature of 550 °C was chosen for further experiments based on optimum results obtained, and it is the commonly accepted temperature at which pyrolysis of tires was considered complete [18,22,35–37]. This maximum temperature was held for 1 h in order to ensure that all pyrolytic reactions were completed.

The char was further activated by the PPO process in which 7% oxygen was introduced into the pyrolysis furnace to oxygenate the char, after pyrolysis was completed and the temperature started to decrease. No additional energy was used to maintain a fixed temperature. Instead, the temperature was allowed to fall gradually, as thick thermal insulation was employed around the work tube. The percentage of oxygen fed into the pyrolysis reactor was monitored using a flow meter, with a flow rate ratio of air to nitrogen gas at 1:2. The experimental setup for this process is shown in Fig. 1.

PPO was carried out in the pyrolysis reactor at different temperatures, depending on the start and end temperatures. The oxygenation carried out between the temperatures of 550 °C and 250 °C on chars was named P550250. Likewise, P450400 would refer to chars that were oxygenated from 450 °C to 400 °C, and the same abbreviation for referring to other chars processed at different temperatures. The tire char pyrolyzed in a similar manner, but without oxygenation, is referred to as NoPPO. The activation temperatures and approximate time are listed in Table 1. The chars were removed and weighed for each condition to determine the yield before further analysis. Char yields were expressed as a percentage of the original tire sample weight.

Table 1
Starting and ending activation temperatures and approximate times.

Sample	Starting temperature (°C)	Ending temperature (°C)	Activation time (min)
P550250	550	250	120
P450400	450	400	45
P350300	350	300	50
NoPPO	Nil	Nil	Nil

2.3. Characterization

2.3.1. Proximate analysis

The ASTM D3172-07 method was used in determining the proximate amounts of moisture, volatile matter, ash and fixed carbon for the raw tire, pyrolyzed, unoxygenated char and oxygenated char. The Carbolite CWF 1100 furnace (Sheffield, England) was used, which was capable of heating samples up to 1000 °C.

2.3.2. Bulk metal content

A composite mix of three concentrated chemicals (HNO_3:HF:H_2O_2 = 14:1:4) was used to digest the pyrolyzed chars. The digestion process was assisted by microwave irradiation by placing the mixtures in a microwave (MLS-1200 mega, Milestone s.r.l, Italy) oven at a maximum power of 600 W for 12 min. The digested solutions were diluted and analyzed using inductively coupled plasma–mass spectrometry (ICP–MS, Perkin Elmer Elan 6100 ICP–MS, Perkin Elmer Inc., USA).

2.3.3. X-ray photoelectron spectroscopy

The residue samples were also analyzed using XPS (Kratos AXIS Hsi, from Kratos Inc., UK) for surface elements; and curve-fitting software (XPSEPAK version 4.1) was used to deconvolute the peaks and elucidate the corresponding groups.

2.3.4. Surface area and porosity

For measurements of pore size distributions and BET surface areas, the NOVA 4200 Multi-station Anygas Sorption Analyzer (Quantachrome Instruments) was used. Nitrogen adsorption isotherms were obtained at −196 °C (77 K) and the BET (Brunauer–Emmett–Teller) equation used to obtain the surface areas while the BJH (Barret–Joyner–Halenda) method was used to derive the pore size distribution [33].

2.3.5. Scanning electron microscope (SEM)

Images of the char surfaces were taken with a SEM (JEOL, JSM-5600 LV) at magnifications of 1000×, 3000× and 5000×. The tire samples were dried overnight at 50 °C prior to the electron microscopy.

2.3.6. Equilibrium copper removal studies

For equilibrium experiments, each sample of 100 mg of tire char, with 100 mL of copper solution ($Cu(NO_3)_2$) at 25 mg per L (3.93×10^{-4} mol per L), was shaken for 14 h at a speed of 150 rpm, with the initial pH of the solutions adjusted to 5.0 (±0.2) and at 24 °C (297 K). For each run, at least three samples were used and one flask of the solution without solids was also tested as a blank experiment. The solutions were then filtered off using a 0.45 μm paper filter to remove the solids from the solutions. The copper concentrations before and after adsorption were measured using an inductively coupled plasma–optical emission spectrometry (ICP–OES, Perkin-

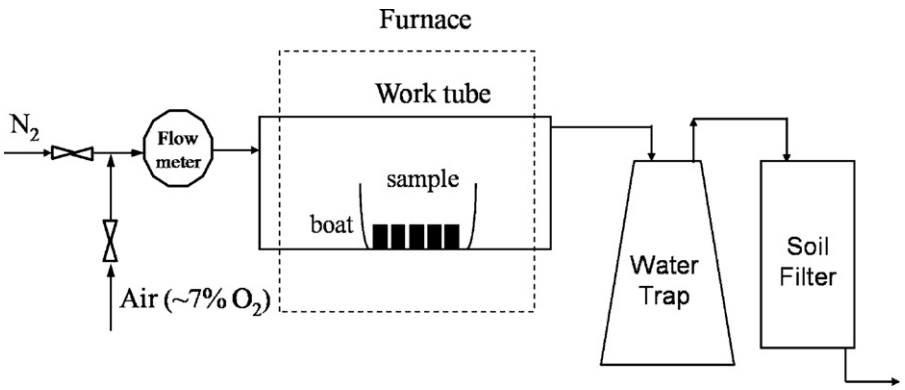

Fig. 1. Experimental setup for the production and activation of pyrolytic char.

Elmer ICP Optima 3000DV) and AAS (Perkin-Elmer Analyst 300) to check that results are not machine-dependent. At least four different concentrations and a blank (DI water) were used for instrumental calibration and for generating a calibration plot.

3. Results and discussion

3.1. SEM images

SEM images of the char surfaces are shown in Figs. 2 and 3. At 1000× magnification (Fig. 2), the oxygenated char showed very different surface morphology as compared to the unoxygenated char. The oxygenated char (P550250) surface was composed of a finer grain surface structure than the unoxygenated char (NoPPO). However, this does not seem to translate to very different surface areas, as presented in Section 3.5.

Fig. 3 shows numerous cracks and fissures on the surface of the oxygenated char. Although these features seem to be mesoporous, they do not seem to contribute significantly to the surface areas of the chars (Section 3.5).

3.2. Proximate analysis

The various weight fractions of the raw tire, pyrolyzed char and oxygenated char are shown in Table 2. For the raw tire, nearly two-thirds of the mass were composed of volatile rubber compounds, while the nearly one-third remained as fixed carbon. The pyrolyzed chars contained mainly fixed carbon and ash, as the pyrolysis process removed nearly all the volatile matter. The ash content remained largely in the char after pyrolysis and oxygenation. This ash content is a measure of the non-volatile and non-combustible component of the chars. No significant differences in the various fractions could be seen in the proximate analysis for the different degrees of oxygenation. Thus from Figs. 2 and 3 and Table 2, it could be seen that the PPO process affected only the surface and not the bulk of the chars.

3.3. Bulk metal content

Table 3 shows the mineral content of the raw tire and pyrolyzed chars. Of the 24 elements analyzed by ICP–MS, only some could be detected and these elements are shown in the. Of these elements, only zinc and the alkaline and alkaline earth metals are considered to be of significance in the adsorption of heavy metals onto the char.

Thus from Table 3, it could be seen that zinc and silicon were the only major inorganic constituents in the tire char, consistent with previous findings [5–8,12,24,25]. Of these elements, Zn is perhaps the more reactive element. The next largest component is calcium, which is added as carbonate during the tire manufacturing process. Previously, XPS measurements by Darmstadt et al. [7] on the inorganic fraction of pyrolytic chars also showed no crystalline compounds on the surface other than those belonging to zinc. Both the carbonates and amphoteric ZnO played a role in moderating the pH of the aqueous environment. This is likely to influence the adsorption capacities of the pyrolytic char and in the adsorption mechanisms [17–22]. The inorganic materials in the chars also affected its surface areas. Subsequent oxygenation and activation were unlikely to change the macrostructures of these fractions. Thus, it is difficult to significantly increase the surface areas of chars with a high proportion of inorganics [25].

3.4. Surface composition by XPS

The char's external surface composition can be seen in a XPS wide scan. Fig. 4 shows the electron emission peaks corresponding to each major atomic species on two different chars' surface. The highest peak is the carbon peak at a binding energy (BE) of 280–295 eV, while the other major species are oxygen (BE, 525–540 eV), the middle peak, and Zn (1021.8–1021.9 eV), at the left side of the spectrum in each figure. No other peaks of any significant size could be detected by this method, indicating that all functional groups of interest were composed of only Zn, O, C, and possibly H atoms. The oxygenated char (P550250) showed stronger peaks, with larger areas, than the unoxygenated char (NoPPO) due to the increased presence of oxygen.

Table 4 gives the surface relative mass concentrations of these 4 elements, as calculated by their peak areas. No strong peaks for nitrogen could be detected (Table 3), indicating a lack of nitrogen groups on the carbon surface, and these groups are thus of no further interest for discussion. The values also strongly indicate that oxygenation of the char does indeed occur, with more oxygen content in the char at a higher temperature range.

More details of each of these three peaks can be obtained by focusing the X-ray beam at these individual peaks. According to earlier researchers [38–40], each functional group has a corresponding BE. Therefore, different curves corresponding to different functional groups were fitted under each of the three highly-resolved peaks, which can give information on the relative amounts of each functional group. Fig. 5 shows the BE peaks for the Zn_{2p} electrons.

The Zn_{2p} peak of atomic zinc at a BE of 1021.8–1021.9 eV and its oxide peak at 1022.5 eV [41] can be used to identify the extent of PPO on the pyrolyzed char. Fig. 5(a) and (b) shows the result of this fit. The char that has been oxygenated (P50250) showed a large oxide peak (Fig. 5(b)) to the left of the main zinc peak, with the oxide peak area larger than the zinc peak. The unoxygenated char (NoPPO) shows almost no oxide peak (Fig. 5(a)). Similar peaks were obtained for C_{1s} and O_{1s} and analyzed for their functional groups.

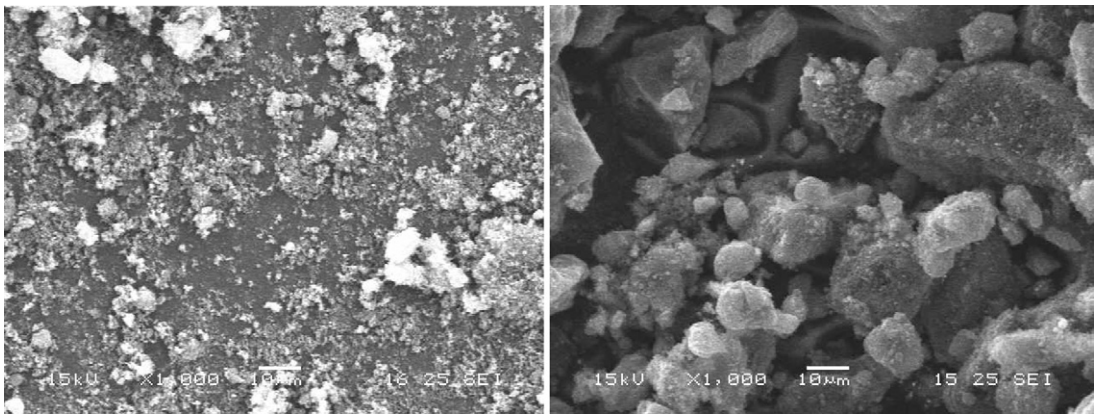

Fig. 2. Oxygenated char (P550250) (left) and unoxygenated char (NoPPO) (right) at 1000× magnification.

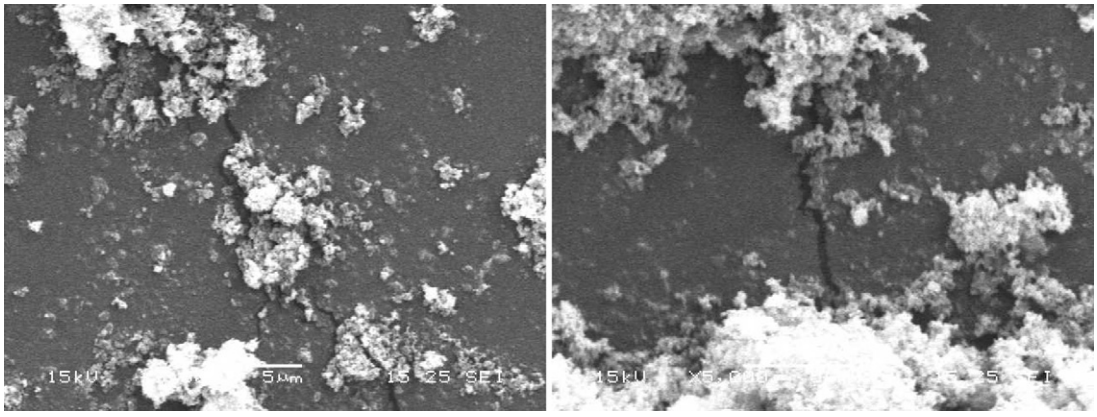

Fig. 3. Oxygenated char (P550250) at 3000× magnification (left) and 5000× magnification (right), showing cracks and fissures.

Table 2
Proximate analysis of feedstock tires.

Fraction	Weight %				
	Raw tire	NoPPO	P350300	P450400	P550250
Volatile matter	63.8 ± 2.50	0.41 ± 0.20	4.54 ± 1.20	4.61 ± 0.93	5.81 ± 1.01
Fixed carbon	32.5 ± 0.25	90.5 ± 11.8	85.6 ± 7.50	85.2 ± 5.40	82.9 ± 6.50
Ash	2.85 ± 0.25	8.63 ± 0.45	9.41 ± 1.92	9.85 ± 1.54	10.9 ± 1.81
Moisture	1.05 ± 0.10	0.46 ± 0.02	0.45 ± 0.05	0.37 ± 0.02	0.39 ± 0.02

The curve fitting for the various peaks to the O_{1s} spectra [39–41] for the two char types revealed that the zinc oxide peak (B.E. 530.4 eV) was much larger for P550250 than for the NoPPO char (530.8 units vs. 24.7 units), as shown in Fig. 6. The oxygenated char also had higher proportions of C–OH and/or C–O–C groups compared to C=O groups. This observation shows a higher degree of saturation and higher oxygen concentration on the surface than the unoxygenated char. Small peaks could also be fitted for chemisorbed oxygen and/or water. However, the presence of water in any significant amount can be ruled out as the samples were

Table 3
Mineral content of the pyrolyzed char and the raw tire.

Element	Weight %				
	Raw tire	NoPPO	P350300	P450400	P550250
Al	0.068 ± 0.015	0.130 ± 0.033	0.152 ± 0.043	0.166 ± 0.050	0.220 ± 0.038
Cu	0.005 ± 0.001	0.008 ± 0.004	0.009 ± 0.005	0.011 ± 0.006	0.017 ± 0.003
Fe	0.030 ± 0.009	0.089 ± 0.022	0.091 ± 0.025	0.125 ± 0.026	0.205 ± 0.078
Si	0.563 ± 0.075	2.662 ± 0.267	2.841 ± 0.307	3.012 ± 0.355	3.766 ± 0.350
Zn	1.024 ± 0.007	2.525 ± 0.452	2.614 ± 0.411	3.224 ± 0.316	3.518 ± 0.353
Ca	0.389 ± 0.068	0.368 ± 0.038	0.389 ± 0.028	0.377 ± 0.036	0.382 ± 0.038
K	0.099 ± 0.019	0.142 ± 0.021	0.153 ± 0.030	0.144 ± 0.016	0.157 ± 0.014
Mg	0.040 ± 0.012	0.086 ± 0.021	0.087 ± 0.029	0.075 ± 0.006	0.117 ± 0.040
Others	0.040 ± 0.056	0.450 ± 0.011	0.550 ± 0.019	0.881 ± 0.018	0.100 ± 0.011
Total	2.259 ± 0.263	6.063 ± 0.867	6.886 ± 0.897	8.015 ± 0.829	8.472 ± 0.928

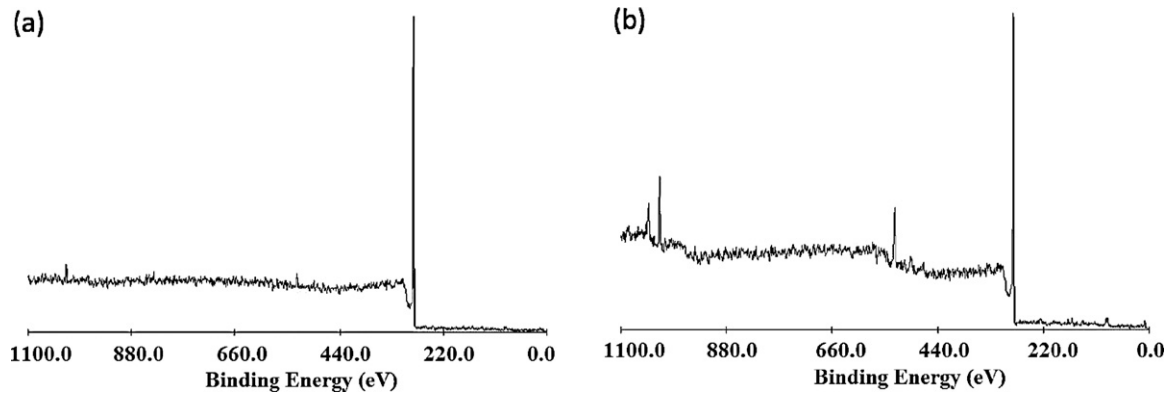

Fig. 4. Wide scan XPS spectrum of pyrolyzed, (a) unoxygenated char (NoPPO) and (b) char oxygenated from 550 °C to 250 °C for 2.5 h using 7% oxygen (P550250).

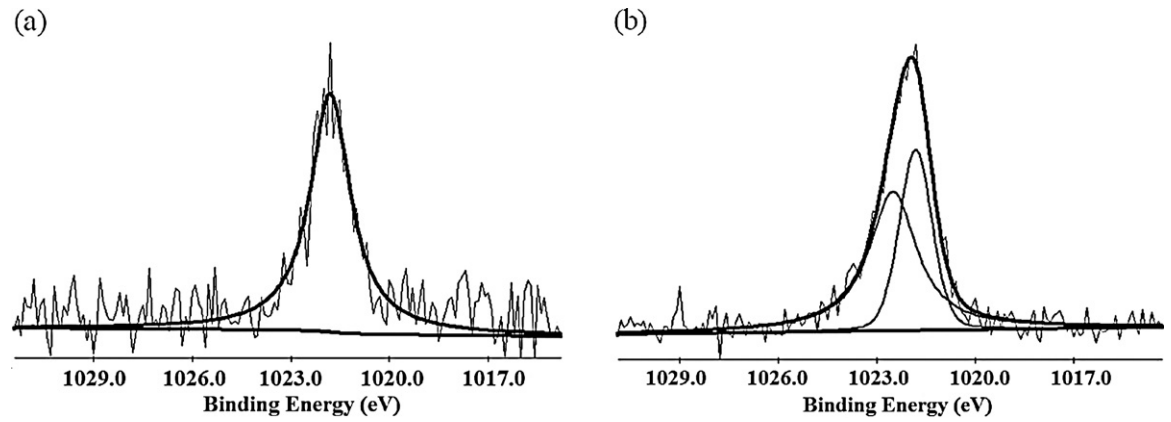

Fig. 5. Zn_{2p} spectra curve fitting for (a) NoPPO char, showing only the main zinc peak, and (b) P550250 char, showing a large oxygen peak in adiition to the zinc peak.

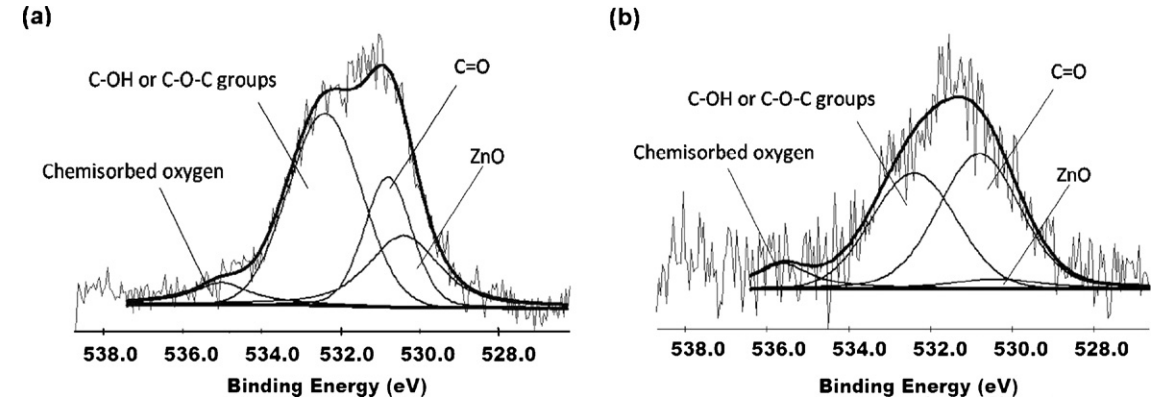

Fig. 6. Oxygen O_{1s} peak (a) for P550250 char (b) for NoPPO char.

dried in the oven prior to XPS analysis, and XPS was also performed under vacuum.

The area under each curve and the percentage of the total area for the oxygen peak are summarized in Table 5. The proportion of ZnO formed through the oxygenation process was more than five times higher for P550250 than for the unoxygenated char. Although the highest proportion of the oxygen was found in the carbon functional groups in both chars, the total amount of oxygenated groups on P550250 was still nearly three times more than that for NoPPO, as given by their respective areas.

Table 4
Quantification of surface elements based on peak areas by XPS.

Char type	Mass concentration (%)			
	Zn	O	C	N
NoPPO	1.57	3.66	94.01	0.76
P350300	4.54	5.78	88.81	0.87
P450400	5.40	6.80	86.82	0.98
P550250	6.79	8.85	83.70	0.65

The C_{1s} spectra provide more details on the carbon functional groups, which are consistent with the evidence provided in earlier sections. Fig. 7 gives a visual representation of the relative peak areas. Generally, the dominant peak is the main graphitic peak, which accounts for a much larger relative area than all other carbon peaks. Chars with different degrees of oxygenation all showed the same dominance by the main graphitic peak (figures not shown). Table 6 shows the assignments and the binding energies for each

Table 5
Assigned oxygen groups' binding energies and respective relative areas.

	Binding energies (eV)	P550250		NoPPO	
		Area (units)	% of total units	Area (units)	% of total units
ZnO	530.4	360.76	22.38	24.691	4.32
C=O	530.8	369.23	22.90	274.75	48.02
C–OH/C–O–C	532.4	776.17	48.14	225.93	39.48
Chemisorb oxygen	535.6	106.16	6.58	46.835	8.19
Total	–	1612.3	100.00	572.20	100.00

Table 6
Assigned groups' binding energies and respective relative areas.

Assigned group(s)	Binding energies (eV)	Relative area (%)			
		NoPPO	P350300	P450400	P550250
$\pi-\pi^*$transitions in aromatics	291.2–292.1	5.176	1.485	2.978	7.681
COOH, COOR	289.3–290.0	1.797	2.001	2.335	5.755
Carbonyl C=O	287.5–288.1	1.575	3.960	4.611	4.587
C–O, C–O–C	286.3–287.0	8.827	9.877	9.617	22.82
Main graphitic peak	284.6–285.1	100.0	100.0	100.0	100.0
Carbidic	282.6–282.9	0.076	0.002	0.323	0.174

peak, together with the normalized peak areas compared to the main graphitic peak. Oxygenation at higher temperatures increased oxygen functional groups, as indicated by the relative sizes of the peaks. P550250 char showed the most significant increase, with highest amounts of the oxygenated group. This increase was due to the lower activation energies required to form a single bond compared to a double bond. The carbidic carbon peak areas were consistently low in all cases and were not therefore considered to be present in amounts that could significantly affect the char's surface chemistry.

Darmstadt et al. [6,7] pyrolyzed used tires under vacuum [6] and atmospheric pressure and compared them to commercial carbon blacks [6,7] and ZnO covered with carbonaceous deposits [7]. Their results showed that commercial carbon black consisted almost entirely of carbon on its surface, while vacuum pyrolytic tire char contained oxygen, nitrogen, sulfur and zinc [6,7]. By comparison, the absence of nitrogen and sulfur peaks in this work was due to the oxygenation process, which reduced these surface atoms to undetectable levels through oxidation. Darmstadt et al. also found that the pyrolytic carbon formed during pyrolysis changed the chemical nature and morphology of the surface [7], with atmospheric pyrolysis having a higher amount of pyrolytic carbon than vacuum pyrolysis. Similarly, the PPO process increased the aromatic carbon content and the surface oxygen functional groups (Tables 5 and 6). Tire chars with carbon-coated zinc also had the greatest variety of carbon functional groups [7], indicating that the presence of zinc and oxygen together could improve the variety of carbon–oxygen functional groups. PPO was also observed to increase the carbon–oxygen groups in this work.

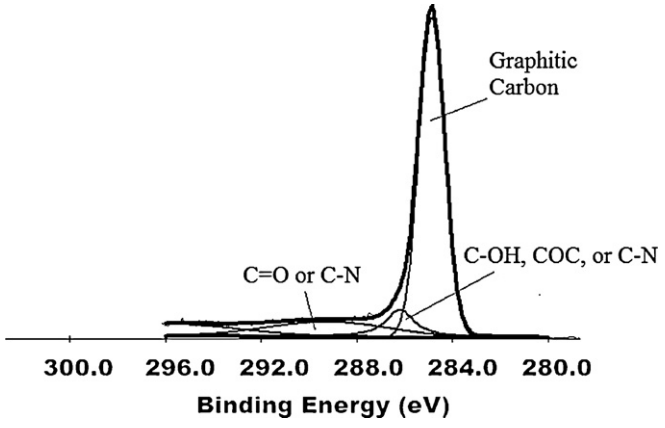

Fig. 7. Carbon C_{1s} peak for P550250 tire char.

It is thus evident that the PPO of tire char without any additional heat can enhance the oxygen content in significant amounts onto the char surface. These oxygenated groups would be beneficial to active carbons to be used for sorption of contaminants. Boehm [34] reported that many properties of carbon materials, in particular their wetting and adsorption behavior, were decisively influenced by chemisorbed oxygen [34]. It is this adsorptive property that allows activated carbon to be used in applications such as air pollution and wastewater treatment.

The XPS data shown in this work revealed that during tire char activation with oxygen or air, a fair amount of oxygen was sorbed onto the surface, forming functional groups and incorporating them into the char. Thus, oxidation of pyrolytic tire char is a dynamic attrition/sorption process. The zinc present on the char surface also adsorbed oxygen into its structure. However, this sorption of oxygen is unlikely to affect its physical properties, such as surface areas, but is expected to affect its chemical properties [26].

3.5. Surface areas and pore volumes

The average values of the BET surface areas and micro- and mesopore volumes according to the nitrogen isotherms are shown in Table 7. A casual observation of the data seems to show an increasing trend of surface areas with increasing burn-off [12,23]. A maximum value for the surface area was found at P550500, corresponding to the lowest yield. Suuberg and Aarna [12] have found that there was a portion of active carbons on carbon surfaces that was more reactive than the rest. This reactive portion, accounting for 23% of the total carbon material, would be removed preferentially when the char is activated in an oxidizing environment, such as oxygen or air [12]. Similarly, Lin and Teng [23] found maximum surface area of tire char at 43% burn-off when activated in steam. They attributed the increase in surface areas to removal of carbon residues retained in inter-aggregate voids during the carbonization process. The removal of carbon residues can explain the almost 100% increase in surface areas when the char activation starts at 500 °C and above in this case (Table 7). It is also apparent from Table 7 that significant burn-offs were achieved only above 500 °C, with a 8.2% burn-off for P550250, but only 2.5% and 2.8% burn-offs for P450400 and P350300, respectively. These values are in agreement with Heras et al. [42], who activated tire chars using a cyclic

Table 7
Surface areas and pore size distribution of chars with various degree of oxygenation.

	Surface Area (m^2/g)	Micropore volume (cm^3/g)	Mesopore volume (cm^3/g)	Average micropore diameter (nm)	Average mesopore diameter (nm)	Yield (%)	Burn-off (%)
P550250	74	0.04	0.33	1.61	28.37	32.5	8.2
P450400	50	0.02	0.22	1.86	27.97	34.4	2.8
P350300	47	0.02	0.19	1.66	27.91	34.5	2.5
NoPPO	72	0.03	0.24	1.63	16.82	35.4	–

chemisorption–desorption process, achieved 2–3% burn-off for the first cycle. They achieved more than 8% burn-off only after the seventh cycle of oxygenation at 550 °C. They also achieve BET surface areas of between 50 and 60 m^2/g after their first cycle, similar to the surface areas found in this work.

The lower degree of burn-offs compared to previous findings also explains the almost identical pore sizes regardless of activation conditions, as gasification of residues may not occur easily at lower temperatures, especially at temperatures lower than the carbonization temperature. Darmstadt et al. [6] observed no significant differences in BET surface areas of chars pyrolyzed under vacuum from 420 to 700 °C. They also found no dependence on the surface composition with surface area or structure. Suuberg and Aarna [12] also found little difference in porosity development with temperature in the range of 400–500 °C under oxygen activation. There is also a significant loss in microporosity only after 39% burn-off [12]. These findings are in agreement with the observations made in this study. In addition, Lin and Teng [23] also found that tire chars are mesoporous while commercial activated carbon is microporous. There would thus be very little change in the mesopores of tire char under these circumstances as well, as shown in Table 7.

The XPS evidence presented earlier showed that oxygen was adsorbed onto the char during activation. The temperature range of activation influenced the amount of oxygen adsorbed, as well as the carbon evolved, as commonly indicated by the yield or burn-off [1,33]. There are thus two apparently conflicting outcomes when oxygen interacts with the carbon surface during activation at temperatures below their pyrolysis temperature: adsorption onto the surface and forming part of the solid structure and the removal of carbon from the surface through gasification. Such adsorption/gasification phenomenon was shown to occur on graphite surfaces, with a possible scheme of reactions, by Best et al. [43] more than two decades ago. Thus, it is possible for the unoxygenated char to have a surface area that is higher that chars oxygenated at lower temperature ranges. The process of oxygen sorption occurring on surface pores, lattice edges and corners, without a corresponding evolution of carbon off the surface, may have the net effect of reducing its physical surface area.

It must also be noted that there are also large deviations from these values among the samples measured on the order of ±20 m^2/g. Therefore, any variation in porosities and BET surface areas should consider the non-homogeneity of pyrolyzed tire char. Huge variations in surface areas and pore volumes of tire pyrolytic char are also supported by the literature, with surface areas of 19–93 m^2/g [6,11,12,14–19]. Therefore, variations in tire char surface areas could be a result of the dynamic processes of oxygen adsorption and carbon gasification on the surface and are dependent on the reactivity of the char surface and the temperature of oxygenation.

3.6. Copper removal results and correlation with char characteristics

The amounts of aqueous copper removed by the various chars are presented in Figs. 8 and 9. It can be seen from the figures that the higher the extent of oxygenation, the higher the removal of copper from solution. However, oxygen functional groups were not found to be solely responsible for aqueous copper removal. Fig. 8 shows the correlation between the amount of zinc and oxygen atoms on the surface of the char and the amount of copper removed per unit mass of the char. Zinc showed a much higher correlation to the amount of copper removed ($R^2 > 0.99$) than oxygen, although both surface elements together also showed good correlation. This is because the ZnO functional group is believed to play an important role in the removal of copper ions from solution [44]. Other functional groups, such as carbon–oxygen functional groups are also believed to play a role in the sorption of copper ions, although their correlation could not be ascertained (data not shown).

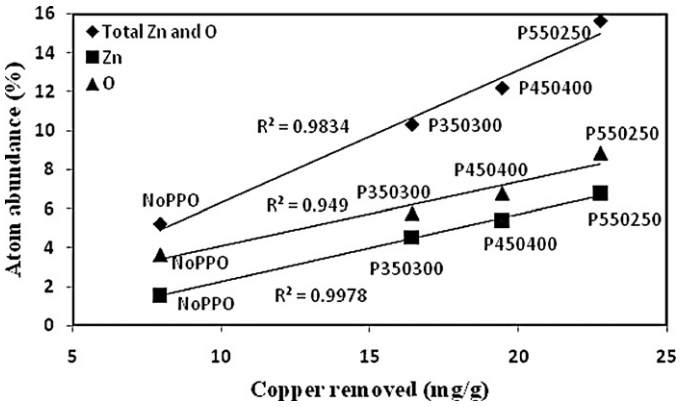

Fig. 8. Correlation of copper removal with surface elements.

Fig. 9 shows the poor correlation between surface areas, pore volumes and the amount of aqueous copper removed. An earlier work [44] showed that the primary copper removal mechanism was by precipitation and adsorption. However, since only a small proportion of the surface (<16%) was covered with Zn and O functional groups, as shown in Fig. 8, the total surface area may not be correlated with the copper removal. Pore diffusion also accounts for less than 19% of the total removal [44]. Rather, it is the total amount of functional groups on the surface that is the single most

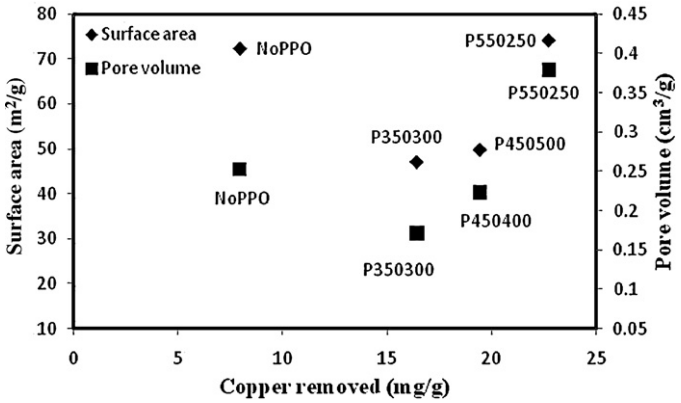

Fig. 9. Correlation of copper removal with surface areas and pore volumes.

significant factor in influencing copper removal. Surface chemistry, rather than physical surface area, is the dominant mechanism for copper removal.

4. Conclusions

This study showed that pyrolyzed chars can be activated by air without the addition of any energy or chemicals, and without significant mass losses. The pyrolyzed tire char adsorbed oxygen with low burn-off. Such a process for pyrolytic char production reduced the costs of feedstocks, input energy and increases the product yield. However, since scrap tires were a form of urban waste, such tire char usage would be restricted to applications of less stringent purity requirements, for example, wastewater treatment or pre-treatment.

Several characteristics of oxygenated pyrolytic tire char were presented. PPO increased the oxygen content on the char surfaces significantly. The PPO process can be used in the production of active sites through the formation of functional groups. These oxygen surface functional groups are considered beneficial to an adsorbent's performance.

The char ash also contained a high amount of metals and minerals. However, only ZnO could be detected by XPS on the surface of the tire char, with the major element being carbon. Thus, any changes in surface areas were predominantly due to changes in the carbon structure. At higher burn-offs, lower yields and higher surface areas were found in agreement with findings from previous works reported in the literature.

Lastly, a simulated use of chars for wastewater treatment was carried out with the batch removal of aqueous copper from solution, with higher copper removals from chars that are more highly oxygenated. Copper removal was correlated highly with zinc ad oxygen surface atom abundance, but not with BET surface areas and pore volumes, indicating that surface chemistry was more important than surface areas in copper removal.

References

[1] R.C. Bansal, M. Goyal, Activated Carbon Adsorption, Taylor & Francis Group LLC, Boca Raton, 2005.
[2] The Freedonia Group, World activated carbon – forecasts for 2012 and 2017 in 17 countries, The Freedonia Group Inc., Study #2363, 2008.
[3] M. Beecham, Global market review of automotive tyres – forecasts to 2014, Aroq Limited, UK, 2008.
[4] E.L.K. Mui, D.C.K. Ko, G. McKay, Production of active carbons from waste tyres – a review, Carbon 42 (2004) 2789–2805.
[5] D.C.K. Ko, E.L.K. Mui, K.S.T. Lau, G. McKay, Production of activated carbons from waste tire – process design and economical analysis, Waste Manage. 24 (2004) 875–888.
[6] H. Darmstadt, C. Roy, S. Kaliaguine, Characterization of pyrolytic carbon blacks from commercial tire pyrolysis plants, Carbon 33 (1995) 1449–1455.
[7] H. Darmstadt, C. Roy, S. Kaliaguine, ESCA characterization of commercial carbon blacks and of carbon blacks from vacuum pyrolysis of used tires, Carbon 32 (1994) 1399–1406.
[8] J.A. Conesa, I. Martin-Gullon, R. Font, J. Jauhiainen, Complete study of the pyrolysis and gasification of scrap tires in a pilot plant reactor, Environ. Sci. Technol. 38 (2004) 3189–3194.
[9] A. Lucchesi, G. Maschio, Semi-active carbon and aromatics produced by pyrolysis of scrap tires, Conserv. Recycl. 3 (1983) 85–90.
[10] C.S. Yuan, H.Y. Lin, C.H. Wu, M.H. Liu, C.H. Hung, Preparation of sulfurized powdered activated carbon from waste tires using an innovative compositive impregnation process, J. Air Waste Manage. Assoc. 54 (2004) 862–870.
[11] G. San Miguel, G.D. Fowler, C.J. Sollars, A study of the characteristics of activated carbons produced by steam and carbon dioxide activation of waste tyre rubber, Carbon 41 (2003) 1009–1016.
[12] E.M. Suuberg, I. Aarna, Porosity development in carbons derived from scrap automobile tires, Carbon 45 (2007) 1719–1726.
[13] W. Kaminsky, C. Mennerich, Pyrolysis of synthetic tire rubber in a fluidized-bed reactor to yield 1,3-butadiene, styrene and carbon black, J. Anal. Appl. Pyrolysis 58–59 (2001) 803–811.
[14] H. Teng, Y.C. Lin, L.Y. Hsu, Production of activated carbons from pyrolysis of waste tires impregnated with potassium hydroxide, J. Air Waste Manage. Assoc. 50 (2000) 1940–1946.
[15] P. Ariyadejwanich, W. Tanthapanichakoon, K. Nakagawa, S.R. Mukai, H. Tamon, Preparation and characterization of mesoporous activated carbon from waste tires, Carbon 41 (2003) 157–164.
[16] H.Y. Lin, W.C. Chen, C.S. Yuan, C.H. Hung, Surface functional characteristics (C, O, S) of waste tire-derived carbon black before and after steam activation, J. Air Waste Manage. Assoc. 58 (2008) 78–84.
[17] K. László, L.A. Bóta, G. Nagyu, Characterization of activated carbons from waste materials by adsorption from aqueous solutions, Carbon 35 (1997) 593–598.
[18] R. Helleur, N. Popovic, M. Ikura, M. Stanciulescu, D. Lin, Characterization and potential applications of pyrolytic char from ablative pyrolysis of used tires, J. Anal. Appl. Pyrolysis 58–59 (2001) 813–834.
[19] N.K. Hamadi, X.D. Chen, M.M. Farid, M.G.Q. Lu, Adsorption kinetics for the removal of chromium(VI) from aqueous solution by adsorbents derived from used tyres and sawdust, Chem. Eng. J. 84 (2001) 95–105.
[20] F. Rozada, M. Otero, A.I. García, A. Morán, Application in fixed-bed systems of adsorbents obtained from sewage sludge and discarded tyres, Dyes Pigments 72 (2007) 47–56.
[21] F. Rozada, M. Otero, A. Morán, A.I. García, Activated carbons from sewage sludge and discarded tyres: production and optimization, J. Hazard. Mater. B124 (2005) 181–191.
[22] G. San Miguel, G.D. Fowler, C. Sollars, Pyrolysis of tire rubber: porosity and adsorption characteristics of the pyrolytic chars, J. Ind. Eng. Chem. Res. 37 (1998) 2430–2435.
[23] Y.-R. Lin, H. Teng, Mesoporous carbons from waste tire char and their application in wastewater discoloration, Microporous Mesoporous Mater. 54 (2002) 167–174.
[24] A.A. Zabaniotou, G. Stavropulos, Pyrolysis of used automobile tires and residual char utilization, J. Anal. Appl. Pyrolysis 70 (2003) 711–722.
[25] A. Chaala, H. Darmstadt, C. Roy, Acid-base method for the demineralization of pyrolytic carbon black, Fuel Process. Technol. 46 (1996) 1–15.
[26] A. Quek, R. Balasubramanian, Low-energy and chemical-free activation of pyrolytic tire char and its adsorption characteristics, J. Air Waste Manage. Assoc. 59 (2009) 747–756.
[27] A.M. Cunliffe, P.T. Williams, Composition of oils derived from the batch pyrolysis of tyres, J. Anal. Appl. Pyrolysis 44 (1998) 131–152.
[28] C. Berrueco, E. Esperanza, F.J. Mastral, J. Ceamanos, P.J. García-Bacaicoa, Pyrolysis of waste tyres in an atmospheric static-bed batch reactor: analysis of the gases obtained, J. Anal. Appl. Pyrolysis 74 (2005) 245–253.
[29] W. Kaminsky, C. Mennerich, Pyrolysis of synthetic tire rubber in a fluidized-bed reactor to yield 1,3-butadiene, styrene and carbon black, J. Anal. Appl. Pyrolysis 58 (2001) 803–811.
[30] X. Dai, X. Yin, C. Wu, W. Zhang, Y. Chen, Pyrolysis of waste tires in a circulating fluidized-bed reactor, Energy 26 (2001) 385–399.
[31] G. Lopez, M. Olazar, M. Amutio, R. Aguado, J. Bilbao, Influence of tire formulation on the products of continuous pyrolysis in a conical spouted bed reactor, Energy Fuels 23 (2009) 5423–5431.
[32] S. Galvagno, S. Casu, T. Casabianca, A. Calabrese, G. Cornacchia, Pyrolysis process for the treatment of scrap tyres: preliminary experimental results, Waste Manage. 22 (2002) 917–923.
[33] J.W. Patrick, Porosity in Carbons: Characterization and Applications, Halsted Press, New York, 1995.
[34] H.P. Boehm, Surface oxides on carbon and their analysis: a critical assessment, Carbon 2 (2002) 145–149.
[35] J.H. Chen, K.S. Chen, L.Y. Tong, On the pyrolysis kinetics of scrap automotive tires, J. Hazard. Mater. 84B (2001) 43–55.
[36] P.T. Williams, S. Besler, Pyrolysis–thermogravimetric analysis of tyres and tyre components, Fuel 9 (1995) 1277–1283.
[37] A. Quek, R. Balasubramanian, An algorithm for the kinetics of tire pyrolysis under different heating rates, J. Hazard. Mater. 166 (2009) 126–132.
[38] C. Moreno-Castilla, M.V. Lopez-Ramon, F. Carrasco-Marın, Changes in surface chemistry of activated carbons by wet oxidation, Carbon 38 (2000) 1995–2001.
[39] C.D. Wagner, W.M. Riggs, C.E. Davis, J.P. Moulder, Handbook of X-ray Photoelectron Spectroscopy, Perkin-Elmer Corp, Eden Prairie, 1979.
[40] C.D. Wagner, D.A. Zatko, R.H. Raymond, Use of the oxygen Kllauger lines in identification of surface chemical states by electron spectroscopy for chemical analysis, Anal. Chem. 52 (1980) 1445–1451.
[41] S. Biniak, G. Szymanski, J. Siedlewski, A. Swiatkowski, The characterization of activated carbons with oxygen and nitrogen surface groups, Carbon 35 (1997) 1799–1810.
[42] F. Heras, N. Alonso, M.A. Gilarranz, J.J. Rodriguez, Activation of waste tire char upon cyclic oxygen chemisorption–desorption, Ind. Eng. Chem. Res. 48 (2009) 4664–4670.
[43] J.V. Best, W.J. Stephen, A.J. Wickham, Radiolytic graphite oxidation, Prog. Nucl. Energ. 16 (1985) 127–178.
[44] A. Quek, X.-S. Zhao, R. Balasubramaniam, Mechanistic insights into copper removal by pyrolytic tire char through equilibrium studies, Ind. Eng. Chem. Res. 49 (2010) 4528–4534.